Title
CAPABILITIES OF EARTH-BASED RADAR FACILITIES FOR NEAR-EARTH ASTEROID OBSERVATIONS

Journal
The Astronomical Journal, 152(4)

ISSN
0004-6256

Authors
Naidu, Shantanu P
Benner, Lance AM
Margot, Jean-Luc
et al.

Publication Date
2016-10-03

DOI
10.3847/0004-6256/152/4/99

Peer reviewed

Draft version April 6, 2016
Preprint typeset using LaTeX style AASTeX6 v. 1.0

CAPABILITIES OF EARTH-BASED RADAR FACILITIES FOR NEAR-EARTH ASTEROID OBSERVATIONS

Shantanu. P. Naidu[1], Lance. A. M. Benner[1], Jean-Luc Margot[2], Michael. W. Busch[3], Patrick. A. Taylor[4]

[1]Jet Propulsion Laboratory, California Institute of Technology, Pasadena, CA 91109-8099, USA
[2]Department of Earth, Planetary, and Space Sciences, University of California, Los Angeles, CA 90095, USA
[3]SETI Institute, Mountain View, CA, 94043, USA
[4]Arecibo Observatory, Universities Space Research Association, Arecibo, Puerto Rico, 00612, USA

ABSTRACT

We evaluated the planetary radar capabilities at Arecibo, the Goldstone 70 m DSS-14 and 34-m DSS-13 antennas, the 70-m DSS-43 antenna at Canberra, the Green Bank Telescope, and the Parkes Radio Telescope in terms of their relative sensitivities and the number of known near-Earth asteroids (NEAs) detectable per year in monostatic and bistatic configurations. In the 2015 calendar year, monostatic observations with Arecibo and DSS-14 were capable of detecting 253 and 131 NEAs respectively. Combined, the two observatories were capable of detecting 276 unique NEAs. Of these, Arecibo detected 95 and Goldstone detected 39, or 38% and 30% the numbers that were possible. This indicates that a substantial number of potential targets are not being observed. The bistatic configuration with DSS-14 transmitting and the Green Bank Telescope receiving was capable of detecting about 195 NEAs, or $\sim 50\%$ more than with monostatic observations at DSS-14. Most of the detectable asteroids were targets-of-opportunity that were discovered less than 15 days before the end of their observing windows. About 50% of the detectable asteroids have absolute magnitudes > 25, which corresponds diameters $<\sim$30 m.

1. INTRODUCTION

Ground-based radar is an invaluable tool for improving the orbits and characterizing the physical properties of near-Earth asteroids (NEAs). Such characterization is essential for identifying and mitigating impact threats, planning robotic and human space missions, and for our scientific understanding of asteroids. Radar range and Doppler measurements of NEAs often have fractional precision better than 1 in 10^7, which can provide dramatic improvements to asteroid orbits, prevent loss of newly-discovered objects, and increase the window of reliable predictions of trajectories by decades to centuries (Ostro and Giorgini 2004). In some cases, signal-to-noise ratios (SNRs) are high enough to obtain delay-Doppler images of the objects with range resolutions as fine as 1.875 m. Delay-Doppler images provide a powerful technique to see surface features, obtain shape models (e.g., Naidu et al. 2013), discover natural satellites (e.g., Margot et al. 2002), and estimate masses and densities from binary systems (e.g., Ostro et al. 2006; Naidu et al. 2015; Margot et al. 2015) and from non-gravitational accelerations due to the Yarkovsky effect (e.g., Benner et al. 2015; Vokrouhlick et al. 2015). Radar observations also help support spacecraft missions such as NEAR-Shoemaker, Hayabusa, Chang'e 2, EPOXI, OSIRIS-REx, and the Asteroid Redirect Mission (ARM).

In 2005, the United States Congress passed the George E. Brown, Jr. Act that directed NASA to detect, track, and characterize near-Earth objects larger than 140 m in diameter. The objectives were based on a National Aeronautics and Space Administration (NASA) report (Near-Earth Object Science Definition Team 2003) which concluded that such objects are capable of penetrating through Earth's atmosphere and causing regional destruction in an impact. In 2010, the goals of the George E. Brown, Jr. act were incorporated in the National Space Policy of the United States of America (https://www.whitehouse.gov/sites/default/files/national_space_policy_6-28-10.pdf) that guides the NASA administrator to pursue capabilities, in cooperation with other departments, agencies, and commercial partners, to detect, track, catalog, and characterize near-Earth objects to reduce the risk of harm to humans from an unexpected impact on our planet and to identify potentially resource-rich planetary objects.

The 305-m Arecibo Observatory in Puerto Rico (2380 MHz, 12.6 cm) and the 70 m DSS-14 antenna at the

Goldstone Deep Space Communications Complex in California (8560 MHz, 3.5 cm) are the only telescopes with radar transmitters that are regularly used to observe NEAs. In 2014, the 34-m DSS-13 antenna at Goldstone was equipped with an 80 kW transmitter that operates at a frequency of 7190 MHz (4.2 cm). The transmitter has a bandwidth of 80 MHz that allows delay-Doppler imaging with range resolutions up to 1.875 m, which is twice as fine as the finest range resolution available with DSS-14's 40 MHz bandwidth transmitter and four times finer than the finest resolution available with Arecibo's 20 MHz bandwidth transmitter. The transmitter at DSS-13 was used to image two NEAs in 2015. The Green Bank Telescope (GBT) is occasionally used in a bistatic configuration to receive radar echoes from NEAs, with DSS-14, DSS-13, or Arecibo transmitting.

In November 2015, the 70-m DSS-43 antenna in Canberra and the 64-m Parkes Radio Telescope obtained the first radar detection of an NEA in Australia with asteroid (413577) 2005 UL5. This is an important capability because these telescopes are located in the southern hemisphere and can point to high southern declinations that cannot be seen by Arecibo, Goldstone, or the GBT. The bistatic DSS-43 to Parkes configuration is currently the most sensitive option for radar observations of NEAs at high southern declinations. Because DSS-43 and Parkes are offset substantially in longitude from Arecibo and Goldstone, they can also allow observations of asteroids at times when targets are below the horizon at the other radar facilities, which could extend rotational coverage for some objects and allow radar observations in Australia that are not possible elsewhere due to scheduling conflicts.

In this paper, we explore the capabilities of these ground-based radars in terms of their relative sensitivities and the number of NEAs detectable per year in various monostatic and bistatic configurations. We seek to answer the question: If resources were not an issue, how many NEAs could be observed with current radar facilities per year? This study is important for strategic planning of observations, implementing policies, and future upgrades.

The first study into this topic was by Jurgens and Bender (1977), who found that 60 out of the 1984 then-known asteroids (near-Earth and main belt) were detectable at either Goldstone or Arecibo over a period of ten years between 1977 and 1987. The number of known asteroids has grown tremendously since then and the number of objects detectable by these facilities is now dramatically higher.

In 2010, the National Research Council, at the request of NASA, conducted a study that found that planetary radar plays a crucial role for achieving the goals of the George E. Brown, Jr. Act (Shapiro et al., 2010). They estimated that about 410 near-Earth Objects could be observed by radar (Arecibo & Goldstone) in a 1-year interval starting in 2008 May. Out of these 140 had been discovered before 2008 May and 270 were found during the time interval considered in the report.

During calendar year 2015, more than 1500 NEAs were discovered (http://minorplanetcenter.net/iau/lists/YearlyBreakdown.html), the largest number of NEA discoveries in a single year. The NEA discovery rate is expected to rise in the next few years as new survey telescopes such as Pan-STARRS 2 and ATLAS become fully operational and new wider-field cameras are installed at the Catalina Sky Survey (CSS) telescopes (Christensen et al., 2015). Because many NEAs are detectable by radar during their discovery apparition (Ostro and Giorgini 2004), 2015 provides the most accurate indication of the number of radar-detectable NEAs under current circumstances. Often the discovery apparition provides the best opportunity for radar observations for decades (Ostro and Giorgini 2004) and considerable effort is devoted to observe such targets-of-opportunity (TOOs). For example, in 2015, 45 TOOs were observed with Arecibo and 15 TOOs were observed with DSS-14.

2. METHODS

We performed an automated search of all NEAs listed on the Minor Planet Center (MPC) website (http://www.minorplanetcenter.net/iau/lists/MPLists.html) that were discovered before the end of 2015 to identify all radar observing opportunities in that year. We downloaded trajectories of the NEAs from the Jet Propulsion Laboratory's Horizons ephemeris service (http://ssd.jpl.nasa.gov/?horizons_doc). We estimated radar SNRs for reception at Arecibo, DSS-13, DSS-14, DSS-43, Parkes, and the GBT for this study. For each telescope, we created a short list of objects that came within 1 astronomical unit (au) of Earth and passed through the declination window of the telescope (Table 1). In this step, we computed the positions of the objects at 1-hour intervals throughout 2015. For each object in the short-list, detailed observing windows were computed by finding the time intervals in which the asteroid was above the minimum viewable elevation of the telescope (Table 1).

Table 1. Telescope parameter assumptions

	DSS-13	DSS-14	DSS-43	Arecibo	GBT	Parkes
Declination range	-35° to $+90^\circ$	-35° to $+90^\circ$	-90° to $+34.5^\circ$	-1° to $+38^\circ$	-46° to $+90^\circ$	-90° to $+26.5^\circ$
Min. elevation (degrees)	20	20	20	70	5	30.5
Accessible sky fraction (%)	79	79	78	32	86	72
Diameter (m)	34	70	70	305	100	64
Aperture efficiency	0.71	0.64	0.64	0.38	0.71	0.45
				0.17 (X-band)		
Transmitter frequency (MHz)	7190	8560	2290	2380	NA	NA
Transmitter power (kW)	80	450	100	900	NA	NA
System temperature (K)	20	18	NA	23	25	28

For each observing window we computed the minimum range to the target and estimated the SNR of its radar echo as $P_{rx}/\Delta P_{noise}$, where P_{rx} is the power of the received echo and ΔP_{noise} is the standard deviation of the receiver noise. P_{rx} can be estimated using the radar equation (e.g., Ostro 1993),

$$P_{rx} = \frac{P_{tx} G_{tx} G_{rx} \lambda^2 \sigma}{(4\pi)^3 R^4}. \quad (1)$$

Here, P_{tx} is the transmitter power, G_{tx} and G_{rx} are the gain of the transmitting and receiving antennae, λ is the radar wavelength, σ is the radar cross-section of the target, and R is the distance between the target and the reference point of the antenna. For monostatic radar observations, the receiving and transmitting antennae are the same so $G_{tx} = G_{rx}$. Antenna gain, G, is given by $4\pi\eta A_{ant}/\lambda^2$, where η is the aperture efficiency of the antenna and A_{ant} is the geometric area of the antenna.

ΔP_{noise} is given by

$$\Delta P_{noise} = \frac{k T_{sys} \Delta f}{(\Delta t \Delta f)^{\frac{1}{2}}}. \quad (2)$$

Here k is Boltzmann's constant, T_{sys} is the receiver temperature, Δf is the frequency resolution, and Δt is the total integration time of the received signal. The SNR is maximized if Δf is equal to the bandwidth (B) of the echo. Because receiver noise is stochastic in nature, the standard deviation of noise power falls off as the square root of the integration time.

The radar cross-section and echo bandwidth depend on the physical properties of the target and are often unknown. The radar cross section is given by $\sigma = \hat{\sigma} A$, where $\hat{\sigma}$ is the radar albedo and A is the projected area of the target. For a spherical object, echo bandwidth is given by $B = 4\pi D \cos\delta/\lambda P$, where D is the diameter, δ is the sub-radar latitude of the object, λ is the radar wavelength, and P is the spin period of the object. The telescope parameters used for the calculations are provided in Table 1. The relative sensitivities per round-trip light time (RTT), the time for the transmitted signal to reach, reflect off of, and return from the target, for various combinations of transmitter and receiver are given in Table 2.

Table 2. Relative sensitivities of various transmitter-receiver combinations

Transmitter	Receiver	Relative sensitivity
DSS-14	DSS-14	1
	Arecibo	5
	GBT	2.3
	DSS-13	0.3
Arecibo	Arecibo	15
	GBT	5
	DSS-13	0.6
DSS-43	Parkes	0.007
DSS-43 (400 kW)	Parkes	0.03
DSS-13	Arecibo	0.2
	GBT	0.08

NOTE—First column indicates transmitting telescope, second column indicates receiving telescope, and the third column indicates SNR/RTT values normalized to that at DSS-14. Transmitter and receiver parameters are provided in Table 1.

We used the European Asteroid Research Node (earn.dlr.de) database, which is the most thorough and up-to-date database of NEA physical properties,

to obtain estimates of D and P. When a diameter estimate was not available from other measurements, we computed a value for D from the absolute magnitude of the object by assuming a typical S-class optical albedo of 0.18. For objects with unknown rotation periods, we assumed a rotation period of 2.1 hours if the object was larger than 140 m in diameter and 0.5 hours for smaller objects. Spin periods for the vast majority of asteroids greater than 140 m exceed 2.1 hours (Pravec et al. 2002), so this threshold places a conservative lower bound on the SNRs of the larger objects. Smaller asteroids exhibit a range of spin periods, both faster and slower than 2.1 hours, and 0.5 hours is a representative value.

For bistatic observations, the radar signal can be transmitted for the entire duration of the observing window (100% duty cycle). For monostatic observations, the same antenna transmits and receives so the duty cycle of transmission cannot exceed 50% and the total integration time of the radar echo cannot be more than half the time of the observing window. Our calculations also took into consideration the finite time required to switch between the transmitter and receiver, which makes the integration time several seconds less than 50% of the observing window.

We adopted an SNR cutoff of ≥ 30/track for the final list of radar-detectable NEAs. Objects are detectable at lower estimated SNRs but the rate of successful detection is close to 100% above this threshold.

Arecibo schedules monthly "survey nights" to observe as many detectable NEAs, mostly TOOs, as possible in a nominally 8-h block of observing time. During these nights they often target NEAs with SNRs weaker than 30/track. This is tractable because Arecibo radar tracks for single objects are usually short (less than 3 hours) as it can only point within 20 degrees of zenith. If a target is not detected rapidly, a new target, if available, is selected. Asteroids with SNRs < 30/track are infrequently scheduled at Goldstone because telescope is heavily subscribed with spacecraft communications and only asteroids with high probabilities of success are scheduled. Radar tracks at Goldstone are usually much longer than at Arecibo and can, at least in principal, last more than 24 hours for objects at high northern declinations. This implies that it may take an unreasonably long time to achieve low SNRs at Goldstone and it may not be practical to schedule such long tracks. We assume that Canberra and Parkes would only be used for crucial targets that are not visible at other radar facilities so we used a lower threshold of SNR ≥ 15/track for these telescopes.

Our calculations account for the discovery announcement dates of the radar-observable NEAs and excluded targets that were detectable by radar only before their discoveries were announced. For targets discovered by the Catalina Sky Survey (CSS) and Mt. Lemmon Survey we added a typical reporting lag time of 2 days between discovery observation and discovery announcements. For the Panoramic Survey Telescope & Rapid Response System (Pan-STARRS) we added 4 days, and for all other observatories we adopted reporting lag times of 10 days. These typical reporting lag times were estimated by averaging over 790 randomly selected asteroid discovery announcements from 2014 from the MPC website. Figure 1 shows the means and standard deviations of the reporting lag times for various observatories. In this paper, we refer to asteroids that were detectable by radar irrespective of their discovery dates as "potentially detectable". We use the term "detectable" to refer to potentially detectable asteroids whose discoveries were announced before the radar view periods ended.

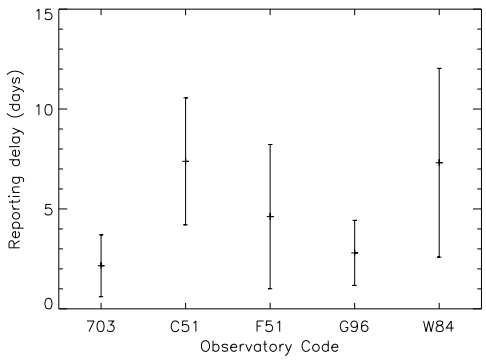

Figure 1. Means and standard deviations of discovery report delays for the top 5 observatories in terms of the number of NEAs discovered. Observatory codes designated by the MPC and sample sizes for each observatory are as follows: 703 Catalina Sky Survey (142), C51 NEOWISE mission (30), F51 PanSTARRS I (320), G96 Mt. Lemmon Survey (263), and W84 Dark Energy Cam (35).

Radar beam sizes are on the order of 1 arcminute, so pointing uncertainties should ideally be significantly smaller than that prior to a radar observation. In practice, we prefer 3σ pointing uncertainties < 20 arcseconds. Radar is not an efficient method for blindly surveying for asteroids due to its narrow beam width and due to the potentially enormous Doppler shifts caused by the object's translational motion. Some known NEAs have large plane-of-sky pointing, Doppler, and time delay uncertainties. For these objects we ignored the uncertainties and adopted the nominal orbit. We often request optical astrometry for such objects so only a few scheduled objects are not detected due to large pointing uncertainties. For some of the observable objects there is insufficient time for scheduling and planning observations before the objects exit the radar windows. More time is required to schedule a target at Goldstone

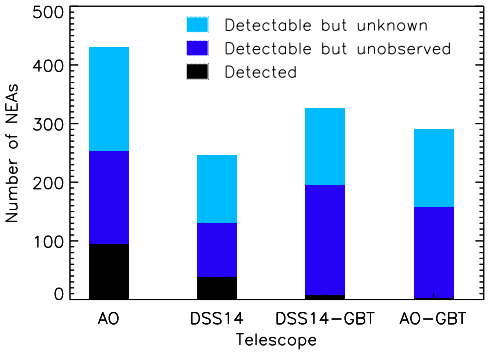

Figure 2. Histogram of currently known NEAs detectable and detected by various configurations of radar telescopes in 2015. AO stands for Arecibo Observatory and DSS-14 is the 70 m antenna at Goldstone. Each bar is divided into three parts: black indicates the asteroids that were observed by radar whereas light and dark blue colors represent asteroids that were not observed by radar. Asteroids in light blue were unknown during their radar observing windows. Dark blue represents asteroids that were known during their radar windows but not observed by radar.

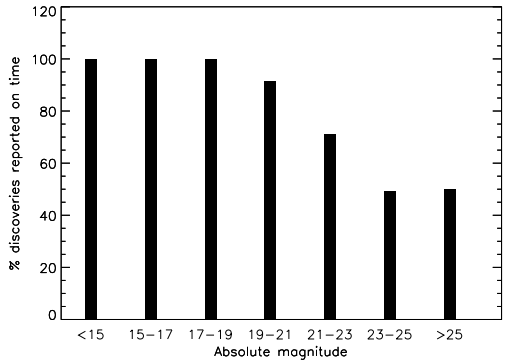

Figure 3. Fraction of potentially detectable asteroids at Arecibo for which discoveries were announced before their radar view periods with SNRs/track > 30 ended.

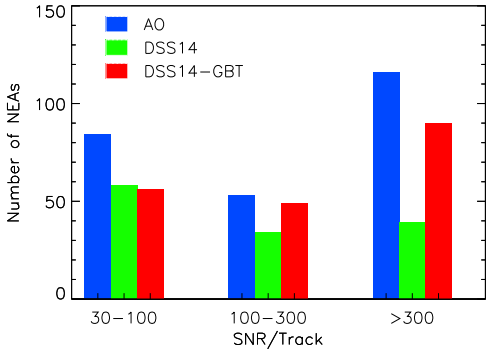

Figure 4. Number of radar-detectable asteroids in the low, medium, and high SNR categories for monostatic observations at Arecibo and DSS-14, and bistatic observations with DSS-14 and Green Bank.

than at Arecibo because obtaining transmit authorization from various government agencies is necessary due to airspace restrictions. Other limitations to schedule NEAs for radar observations include scheduling conflicts with other observing projects, spacecraft communication, equipment problems, and insufficient budget for staffing telescopes to observe all detectable NEAs. DSS-43 and Parkes are currently not configured to observe TOOs on short notices. These limitations make the number of observed targets much lower than the number of detectable asteroids listed in this paper. For Arecibo, DSS-14, and GBT we compared the numbers of observable NEAs with the number of NEAs actually observed.

3. RESULTS

3.1. *Arecibo monostatic*

We found 430 known and new objects that were potentially detectable at Arecibo in 2015 with SNRs greater than 30/track (Figure 2). There were 253 discoveries ($\sim$ 59% of the potentially detectable NEAs) that were announced by the Minor Planet Center before radar view periods with SNR/track $\geq$ 30 ended. The fraction of discoveries announced in time for radar observations varies as a function of the absolute magnitudes of the asteroids as shown in Figure 3. Discoveries of all potentially detectable asteroids brighter than absolute magnitude of 19 were announced before their radar view periods ended. Arecibo detected 95 NEAs in 2015, or about 38% of the NEAs that were detectable.

We divided the population of asteroids detectable by Arecibo into three categories depending on the SNRs/track (Figure 4). The first category consists of asteroids with SNRs/track between 30 and 100 for which we can typically obtain ranging observations and echo power spectra that resolve them in Doppler frequency. There are 84 detectable asteroids in this category (18 were detected). The second category consists of targets with SNRs/track between 100 and 300 that can typically yield delay-Doppler images with coarse to medium resolutions (a few to a few tens of delay pixels over the object). There are 53 detectable asteroids in this category (23 were detected). The third category of targets have SNRs/track > 300. These are imaging targets that can be resolved with range resolutions as fine as 7.5 m/pixel, the highest range resolution available at Arecibo. There are 116 detectable asteroids in this category (36 were detected).

For TOOs that were discovered within 100 days of their radar view periods, Figure 5 shows a histogram of the number of days between discovery announcements and the ends of the observing windows for the corresponding objects. About 80% of new discoveries are detectable by radar only within 15 days of the discovery

announcement. If the delay in reporting NEA discoveries from optical surveys were 2 days for all observatories, then about 270 NEAs would have been detectable at Arecibo, or 17 more than with the current reporting delays. Of the 17 additional targets, 10 are in the highest SNR category. The most notable target among these was the 25-m NEA 2015 SA because of its high SNR/track of ~ 12000.

As we mentioned in section 2, Arecibo sometimes targets NEAs with SNRs < 30/track during survey nights. If we adopt a threshold of SNR/track ≥ 20, then 290 NEAs become detectable at Arecibo, i.e., a 12% increase over the number of detectable asteroids with SNRs ≤ 30/track.

3.2. *DSS-14 monostatic*

We found 246 objects that were potentially detectable at DSS-14 with SNRs/track ≥ 30 in the year 2015 (Figure 2). There were 131 discoveries that were announced on the MPC website before the radar view periods ended. DSS-14 observed 39 NEAs or about 30% of these objects. The targets are roughly evenly spread among the three categories defined in the previous section: 58 targets had SNRs/track between 30 and 100 (10 were detected), 34 had SNRs/track between 100 and 300 (2 were detected), and 39 had SNRs/track greater than 300 that were suitable for high-resolution imaging (Figure 4) (20 were detected). As we found with Arecibo targets, the time between the discovery announcement and the end of the radar window was less than 15 days for most.

Recently an engineering study (L. Teitelbaum, pers. comm.) was conducted to examine the efficacy of doubling the transmitter power at DSS-14 from 450 kW to 900 kW. With such an upgrade, the number of detectable NEAs would have been 165, which is a 26% increase from the current capability. Doubling the transmitter power will also double the SNRs of all detectable NEAs and allow us to image targets with ~ 2 times finer resolution than is possible with current SNRs.

3.3. *Bistatic DSS-14 to Green Bank Telescope*

The number of NEAs detectable by using DSS-14 to transmit and GBT to receive is greater than the NEAs detectable by monostatic DSS-14 observations but less than the number of NEAs detectable with monostatic observations at Arecibo. This is correlated to the collecting area of the receiving telescopes. There were 327 objects that were potentially observable using DSS-14 and GBT in 2015 (Figure 2). There were 195 discoveries that were announced before the end of their radar view periods. This is an increase of 64 radar-detectable asteroids, or about 50%, compared to monostatic observations at DSS-14. The number of NEAs in the highest SNR category (SNR/track ≥ 300) was more than double relative to DSS-14 monostatic observations (Figure 4), indicating that many of the low and medium SNR objects were promoted to the high SNR category. In 2015, we observed 8 NEAs using DSS-14 and GBT. This bistatic configuration was only rarely used for observing NEAs before 2015.

All the objects detectable by DSS-14 monostatically were also detectable using the DSS-14-GBT bistatic configuration mainly due to the similar declination ranges covered by the telescopes. The estimated SNRs were higher in the bistatic configuration because the Green Bank Telescope has a larger effective aperture (100 m vs. 70 m) and the total integration time is about two times greater. On average, the Goldstone (DSS-14) - GBT bistatic configuration provides SNRs/track about 3 times greater than the Goldstone monostatic configuration. Note that this factor compares SNRs/track and is different from the relative sensitivity listed in Table 2, which compares SNRs/RTT.

Lowering T_{sys} at GBT would further increase the relative sensitivity and enable more NEA detections. For example, if T_{sys} were 18 K at GBT, then DSS-14 and GBT would have been able to detect 230 NEAs in a bistatic configuration (compared to 195 NEAs for $T_{sys} = 25$ K). A preliminary study shows that lowering T_{sys} to 18 K at GBT is feasible (J. Ford, personal communication).

There are some limitations to using the DSS-14-GBT bistatic configuration: the GBT isn't always available for radar observations, the latitude and longitude differences means that overlapping time is short for targets at southern declinations, ridges near the GBT restrict useful pointing to elevations > 30 degrees at certain azimuth angles, and weather in the winter can preclude observations.

3.4. *Bistatic Arecibo to Green Bank Telescope*

We found 291 NEAs that were potentially observable with SNRs/track ≥ 30 in 2015 using the Arecibo-GBT bistatic configuration (Figure 2). The discoveries of about 157 of these were reported before the end of their radar view periods. This is fewer than those detectable using DSS-14 and GBT because that configuration provides longer observing windows and results in higher SNRs/track compared to the Arecibo-GBT bistatic configuration for some targets. The number of detectable asteroids is also lower than that for monostatic observations at Arecibo because the GBT has a smaller collecting area than Arecibo. However, the Arecibo to GBT bistatic configuration is very useful because it provides longer integration times and allows for finer Doppler resolution of the data. This is ideal for very close targets with RTT < 10 seconds and/or very slow rotators with intrinsically narrow bandwidths. Three asteroids (2015

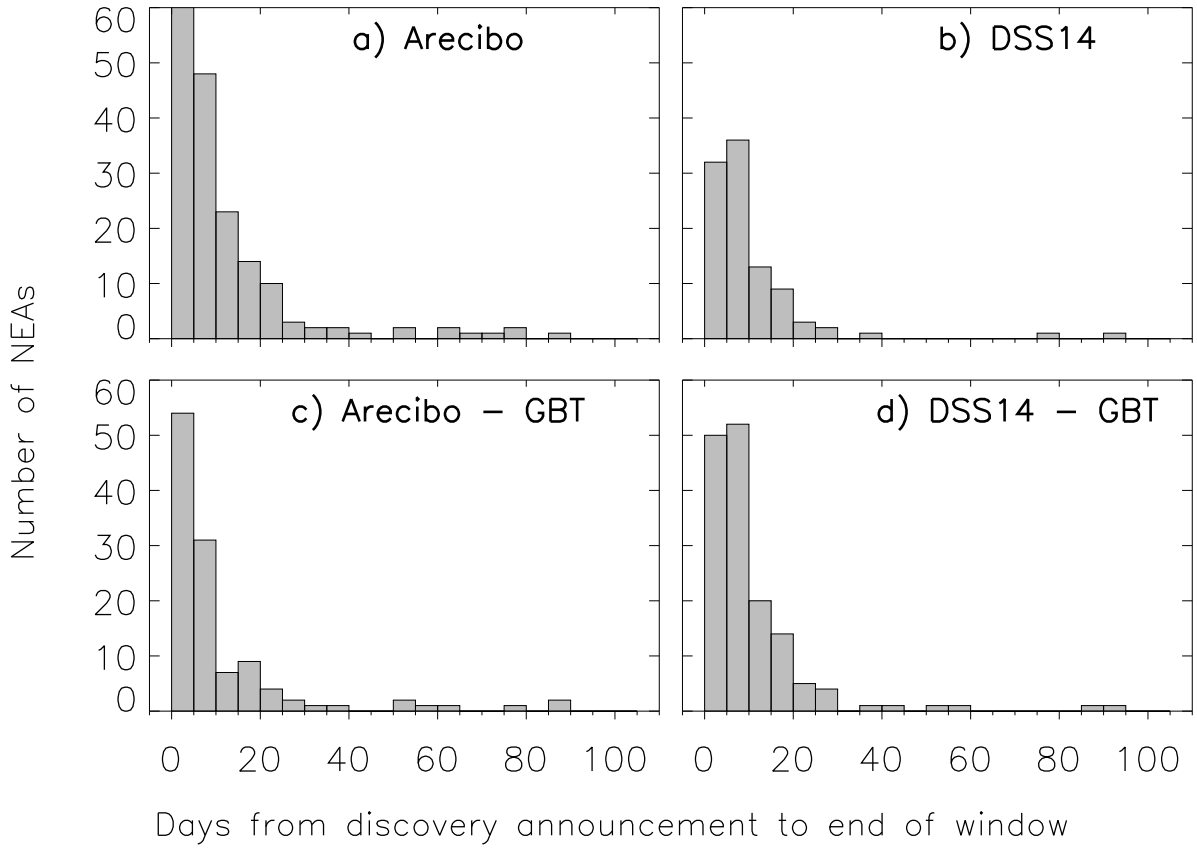

Figure 5. Histograms showing the number of detectable NEAs as a function of the time between discovery announcement to the end of observing window for Arecibo, DSS-14, Arecibo-GBT and DSS-14-GBT.

HM10, 2015 SZ, and 2003 SD220) were detected in this configuration in 2015.

3.5. *Bistatic DSS-13 to Green Bank Telescope*

We found 57 near-Earth asteroids that were potentially detectable with SNRs/track $\geq$ 30 in 2015 using this configuration, and of these, the discoveries of 33 were reported before the end of their radar view periods. Four asteroids were probably strong enough for delay-Doppler imaging with the finest possible range resolution of 1.875 m, namely (357439) 2004 BL86, 2015 HD1, 2015 HM10, 2015 JF1. We observed (357439) 2004 BL86 and 2015 HM10 using this bistatic configuration but we were not able to achieve the maximum range resolution of 1.875 m due to technical difficulties.

NEA (85989) 1999 JD6 was the largest detectable asteroid with a diameter of about 1.8 km and SNR/track of $\sim$ 400. It was detected using DSS-14, Arecibo, and the GBT in 2015 July. The smallest detectable asteroid was 2015 FM118 (SNR/track $\approx$ 700) with an inferred diameter of 5 m based on an absolute magnitude of 28.7. This asteroid approached Earth within 0.002 au in March. At this distance the round-trip light time to the asteroid would have been shorter than the transmit-receive switching time at Arecibo and DSS-14, so bistatic observations would have been the only way to detect this asteroid with radar at the closest approach. The median of the absolute magnitudes of the detectable asteroids was 25.5, which corresponds to a diameter of $\sim$ 24 m.

3.6. *Bistatic DSS-43 to Parkes*

About 70 NEAs were potentially detectable with SNRs/track $\geq$ 15 in 2015 using the bistatic DSS-43 - Parkes configuration. The discoveries of about 34 of these were reported before the end of their radar view periods. Table 3 shows the list of all the NEAs that were observable using this configuration in 2015. One of these asteroids, 2015 BP509, was not observable by any other radar-capable telescopes considered in this paper because its close approach was at a high southern latitude (-36 degrees) which was beyond the reach of telescopes located in the northern hemisphere.

Table 3. NEAs detectable in 2015 using DSS-43 and Parkes

Object	Absolute magnitude	Distance (au)	SNR/track
(33342) 1998 WT24	17.9	0.0280	16
(357439) 2004 BL86	19.3	0.0080	1700
(413577) 2005 UL5	20.3	0.0153	87
(436724) 2011 UW158*	19.9	0.0199	62
2014 YD15	26.8	0.0049	20
2014 YE42	23.4	0.0110	16
2015 BC	24.0	0.0050	300
2015 CL13	25.7	0.0054	44
2015 DS53	24.2	0.0081	37
2015 DY198	26.6	0.0056	30
2015 EF	26.8	0.0065	16
2015 FW117	22.7	0.0092	72
2015 FM118	28.7	0.0031	70
2015 GU	28.4	0.0037	39
2015 GL13	28.8	0.0041	23
2015 HD1	27.4	0.0004	380000
2015 HM10	23.6	0.0039	590
2015 HQ11	27.1	0.0053	20
2015 HO116	25.5	0.0045	150
2015 HQ171*	26.9	0.0052	26
2015 HA177*	27.7	0.0048	24
2015 KW120	26.0	0.0035	300
2015 KA122	23.2	0.0085	63
2015 LF	26.6	0.0014	6000
2015 OQ21*	27.9	0.0040	32
2015 SZ2*	25.4	0.0034	700
2015 TC25*	29.5	0.0013	1600
2015 TB145	20.0	0.0078	4400
2015 VO142*	29.0	0.0026	130
2015 XP	25.8	0.0038	210
2015 XX128*	26.0	0.0062	24
2015 XR169*	28.7	0.0035	35
2015 XY261	27.2	0.0019	2100
2015 YQ1*	28.1	0.0038	39

NOTE—Distance indicates the minimum distance of the asteroid from Earth within the radar observing window. Objects in **bold** were observed by DSS-43 and Parkes. Asterisk (*) indicates that the asteroid is on the NHATS list.

NEA (33342) 1998 WT24 was the largest detectable asteroid in this configuration with a diameter of ~ 400 m (Busch et al. 2008). The maximum SNR/track for this object was about 10-20 in 2015 December, when it approached Earth at a distance of 0.03 au. It was the second asteroid detected by DSS-43 and Parkes after NEA (413577) 2005 UL5. The smallest detectable asteroid was 2015 TC25, with a diameter of 3 m inferred from its absolute magnitude of 29.5. It approached Earth at 0.001 au and its maximum SNR/track was about 1500.

This asteroid was detected by Arecibo in 2015 October, when it was 0.01 au from Earth, 10 times further away than it was at close approach. The median of the absolute magnitudes of all detectable asteroids by DSS-43 and Parkes was 26.6, corresponding to a diameter of 14 m.

Currently the transmitter power at DSS-43 is restricted to less than 100 kW, however it could potentially be raised to 400 kW in the future. With the higher power 62 NEAs (versus 34) would have been detectable using DSS-43 and Parkes. Transmission at higher power would require radiation clearance from government authorities such as local air traffic control, which will increase the time required for scheduling radar observations at DSS-43.

3.7. *Absolute magnitude/size distribution of radar-detectable asteroids*

Figure 6 shows the distribution of absolute magnitudes of the radar-detectable asteroids for each transmitter-receiver configuration. It includes only those objects whose discoveries were announced before their radar view periods ended. For a typical S-class asteroid optical albedo of 0.18, magnitudes of 15, 20, and 25 correspond to diameters of about 3000 m, 300 m, and 30 m respectively but the size of a given object may vary by a factor of two due to albedo assumptions.

The smallest radar-detectable asteroid was 2015 VU64, with an absolute magnitude of 30.6 and a diameter of ~ 2 m. It approached Earth to within 0.0007 au (16.4 Earth radii) and was observable only with a bistatic configuration because the round-trip light time to the asteroid during the radar tracks was less than the transmit-receive switching time at all telescopes. The maximum SNR/track was over 10^6. The largest detectable asteroid was (152679) 1998 KU2, which is ~ 4.6 km in diameter and approached within 0.25 au. It was observable only at Arecibo.

The median of the absolute magnitudes of all radar detectable asteroids is 25.4, which corresponds to a diameter of ~ 25 m. For Arecibo, most of the asteroids fainter than 25 mag fall in the high SNR category, but for Goldstone medium and low SNR targets constitute the majority of the small asteroids. Figure 6 shows that using the GBT as a receiver with DSS-14 promotes all small targets from the medium to the high SNR category. From events such as the meteor airburst over Chelyabinsk in Russia in 2013, caused by an object estimated to be 20 m in diameter (Popova et al. 2013), we now know that even decameter scale objects are capable of causing extensive damage at the local level. To reduce the risk from such events it is important to monitor such asteroids. Many of the small asteroids are also on NASA's Near-Earth Object Human Space Flight Accessible Targets Study (NHATS) list (http://neo.jpl.nasa.gov/nhats/) and could be mission targets in the future. Radar observations can provide key information about and orbit refinement for NHATS objects and thus facilitate future missions.

Out of 1562 NEAs discovered in 2015, $\sim 66\%$ had absolute magnitude > 22 (diameter < 140 m). This explains the high fraction of small radar-detectable asteroids. The means ($\pm$ standard deviations) of the absolute magnitudes of the asteroids observed by Arecibo and DSS-14 are 21.1 ($\pm$ 3.2) and 20.9 ($\pm$ 3.3) respectively. This implies that we are biased towards observing optically brighter asteroids.

4. CONCLUSIONS

Out of the 13513 known NEAs at the end of 2015, about 430 and 246 had SNRs high enough to be detected by Arecibo and Goldstone, respectively, during the calendar year. About 40-50% of these were not observable because their discoveries were reported after the end of their radar observing windows leaving 253 and 131 targets that were actually detectable at Arecibo and Goldstone respectively. Of these, Arecibo and Goldstone observed 38% (95 out of 253) and 30% (39 out of 131). Combined, the two observatories were capable of observing 276 unique NEAs. This number is different from the corresponding value of 410 reported in Shapiro et al. (2010) because we adopted an SNR threshold of 30/track versus 5/track in the earlier study. The analysis in the current study is much more rigorous because we computed detailed SNRs for each object based on the actual close approach circumstances.

Shortening the delay in reporting NEA discoveries from optical surveys would increase the potential of radar observatories. If all the optical surveys reported their discoveries within 2 days, about 17 additional objects, including 10 high SNR objects, become detectable at Arecibo. The bistatic DSS-14 to GBT configuration increases the number of radar-detectable targets by about 50% compared to the monostatic DSS-14 configuration. Most of the low and medium SNR targets in the monostatic case are promoted to the high SNR category, some of which could have been imaged with resolutions as fine as 3.75 m.

This study clearly shows that Arecibo and Goldstone are observing less than one-half of potentially detectable NEAs. The number of NEAs observed by radar could be increased by at least several tens of percent by obtaining more telescope time at Arecibo and Goldstone without changing protocols to respond more rapidly. Most of the radar-detectable asteroids were discovered less than 15 days before their radar observing windows ended and have absolute magnitudes > 25. For Arecibo and Goldstone to observe these targets a more rapid response

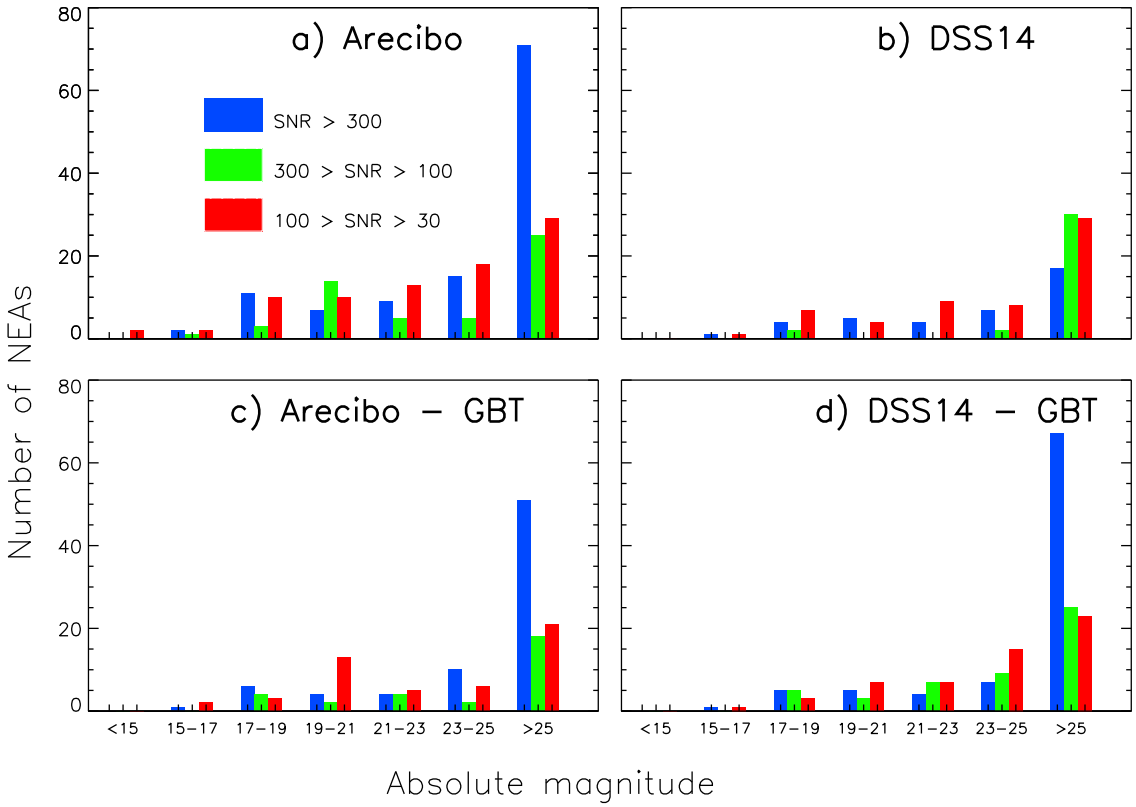

Figure 6. Histogram of the number of radar-detectable NEAs as a function of absolute magnitude for Arecibo (top left), Goldstone (top right), Arecibo-GBT (bottom left) and Goldstone-GBT (bottom right). The targets are divided into high SNR (blue), medium SNR (green), and low SNR (red) targets.

time is necessary at both telescopes and a higher level of dynamic scheduling and staffing that would allow to quickly switching from previously scheduled observations to active radar observations.

This research was conducted at the Jet Propulsion Laboratory, California Institute of Technology, under contract with the National Aeronautics and Space Administration (NASA). The material presented represents work supported by NASA under the Science Mission Directorate Research and Analysis Programs. Part of the work was done at the Arecibo Observatory, which is operated by SRI International under a cooperative agreement with the National Science Foundation (AST-1100968) and in alliance with Ana G. Mndez-Universidad Metropolitana and the Universities Space Research Association. The Arecibo Planetary Radar Program is supported by the National Aeronautics and Space Administration under Grant Nos. NNX12AF24G and NNX13AQ46G issued through the Near Earth Object Observations program.

REFERENCES

L. A. M. Benner, M. W. Busch, Giorgini. J. D., P. A. Taylor, and J. L. Margot. Radar observations of near-earth and main-belt asteroids. In P. Michel, F. E. DeMeo, and W. F. Bottke, editors, *Asteroids IV*. The University of Arizona Press In collaboration with Lunar and Planetary Institute, Tucson Houston, 2015. ISBN 978-0816532131.

R. F. Jurgens and D. F. Bender. Radar detectability of asteroids - A survey of opportunities for 1977 through 1987. *Icarus*, 31: 483–497, August 1977. doi:10.1016/0019-1035(77)90150-6.

J. L. Margot, M. C. Nolan, L. A. M. Benner, S. J. Ostro, R. F. Jurgens, J. D. Giorgini, M. A. Slade, and D. B. Campbell. Binary Asteroids in the Near-Earth Object Population. *Science*, 296:1445–1448, May 2002. doi:10.1126/science.1072094.

J.-L. Margot, P. Pravec, P. Taylor, B. Carry, and S. Jacobson. Asteroid Systems: Binaries, Triples, and Pairs. In P. Michel, F. E. DeMeo, and W. F. Bottke, editors, *Asteroids IV*. The University of Arizona Press In collaboration with Lunar and Planetary Institute, Tucson Houston, 2015. ISBN 978-0816532131.

S. P. Naidu, J.-L. Margot, M. W. Busch, P. A. Taylor, M. C. Nolan, M. Brozovic, L. A. M. Benner, J. D. Giorgini, and C. Magri. Radar imaging and physical characterization of near-Earth Asteroid (162421) 2000 ET70. *Icarus*, 226: 323–335, September 2013. doi:10.1016/j.icarus.2013.05.025.

S. P. Naidu, J. L. Margot, P. A. Taylor, M. C. Nolan, M. W. Busch, L. A. M. Benner, M. Brozovic, J. D. Giorgini, J. S. Jao, and C. Magri. Radar Imaging and Characterization of the Binary Near-Earth Asteroid (185851) 2000 DP107. *AJ*, 150: 54, August 2015. doi:10.1088/0004-6256/150/2/54.

S. J. Ostro. Planetary radar astronomy. *Reviews of Modern Physics*, 65:1235–1279, October 1993. doi:10.1103/RevModPhys.65.1235.

S. J. Ostro and J. D. Giorgini. The role of radar in predicting and preventing asteroid and comet collisions with Earth. In M. J. S. Belton, T. H. Morgan, N. H. Samarasinha, and D. K. Yeomans, editors, *Mitigation of Hazardous Comets and Asteroids*, page 38, 2004.

S. J. Ostro, J.-L. Margot, L. A. M. Benner, J. D. Giorgini, D. J. Scheeres, E. G. Fahnestock, S. B. Broschart, J. Bellerose, M. C. Nolan, C. Magri, P. Pravec, P. Scheirich, R. Rose, R. F. Jurgens, E. M. De Jong, and S. Suzuki. Radar Imaging of Binary Near-Earth Asteroid (66391) 1999 KW4. *Science*, 314: 1276–1280, November 2006. doi:10.1126/science.1133622.

O. P. Popova, P. Jenniskens, V. Emel'yanenko, A. Kartashova, E. Biryukov, S. Khaibrakhmanov, V. Shuvalov, Y. Rybnov, A. Dudorov, V. I. Grokhovsky, D. D. Badyukov, Q.-Z. Yin, P. S. Gural, J. Albers, M. Granvik, L. G. Evers, J. Kuiper, V. Kharlamov, A. Solovyov, Y. S. Rusakov, S. Korotkiy, I. Serdyuk, A. V. Korochantsev, M. Y. Larionov, D. Glazachev, A. E. Mayer, G. Gisler, S. V. Gladkovsky, J. Wimpenny, M. E. Sanborn, A. Yamakawa, K. L. Verosub, D. J. Rowland, S. Roeske, N. W. Botto, J. M. Friedrich, M. E. Zolensky, L. Le, D. Ross, K. Ziegler, T. Nakamura, I. Ahn, J. I. Lee, Q. Zhou, X.-H. Li, Q.-L. Li, Y. Liu, G.-Q. Tang, T. Hiroi, D. Sears, I. A. Weinstein, A. S. Vokhmintsev, A. V. Ishchenko, P. Schmitt-Kopplin, N. Hertkorn, K. Nagao, M. K. Haba, M. Komatsu, T. Mikouchi, and aff34. Chelyabinsk Airburst, Damage Assessment, Meteorite Recovery, and Characterization. *Science*, 342:1069–1073, November 2013. doi:10.1126/science.1242642.

P. Pravec, A. W. Harris, and T. Michalowski. Asteroid rotations. In W. F. Bottke, Jr., A. Cellino, P. Paolicchi, and R. P. Binzel, editors, *Asteroids III*, pages 113–122. University of Arizona Press, Tucson, 2002.

D. Vokrouhlick, W. F. Bottke, S. R. Chesley, D. J. Scheeres, and T. S. Statler. The yarkovsky and yorp effects. In P. Michel, F. E. DeMeo, and W. F. Bottke, editors, *Asteroids IV*. The University of Arizona Press In collaboration with Lunar and Planetary Institute, Tucson Houston, 2015. ISBN 978-0816532131.